

Reply to referee comment 2

The authors deduce subsurface hydraulic properties by an inversion of time-lapse surface GPR measurements during an imbibition experiment of an artificial test site. The coupled inversion process includes a hydraulic simulation by solving the 1D Richards equation and a simulation of radar wave propagation by 2D finite-differences calculation. Water content distribution and electromagnetic soil properties are coupled by a petrophysical relation (CRIM). During the inversion, the misfit between events, i.e. traveltimes and amplitudes of selected reflections, in experimental and synthetic GPR data is minimised. The authors use an inversion scheme that combines several optimisation steps including global and gradient techniques. The approach is first demonstrated for synthetic data and later for experimental data. The result is a 1D subsurface model and for both predefined layers the characteristic hydraulic properties of a Brooks-Corey parameterisation of the water retention function is fitted. The presented work is a relevant contribution towards a non-destructive hydraulic characterisation of the subsurface, which is still an unsolved problem for the unsaturated zone.

Reply: We thank the reviewer for the constructive comments and suggestions. We revised the manuscript accordingly and refer to the revised version in the following.

However, the manuscript has to be overworked as the whole analysis including GPR data processing and inversion is somehow nebulous and difficult to follow. I would also suggest to shorten the text by writing more tersely, avoiding repetitions and possibly moving some parts into an appendix as e.g. GPR data conversion due to Bleistein, details on event detection/association and inversion. Besides this, some major points have to be clarified: 1. Amplitude handling: The formula used for spherical divergence correction for 3D data (P 7 Eq. 10) seems not correct. Correcting with square root of distance is used for 2D data. Also the dimensions of Eq. 10 do not fit. Various formulations of adequate gain functions for 3D (experimental) data is given in Yilmaz: Seismic Data Analysis (2001), e.g. Eq. (1-8a) $g(t) = \frac{v^2(t)t}{v_0^2 t_0}$. The whole amplitude balancing in the manuscript is not clear to me. The radar traces are normalised several times (P8 L1-2) and normalisation is done relative to the maximal absolute amplitude, which is the first reflection. Is the reflector characteristics constant during the entire experiment? What is the advantage of the complicated amplitude adaption due to Bleistein (1986) compared to a simple correction of 2D circular divergence with the square root of the distance? I would suggest

to provide a flow chart of amplitude handling for both experimental (3D) and synthetic (2D) radar data. It seems you use different amplitude handling for event detection and the inversion process?

Reply:

We revised the manuscript, however we decided not to move the GPR evaluation and optimization methods to the appendix since these are actually the essential parts of the manuscript.

Besides an amplitude correction, Bleistein (1986) also provides a correction for the signal frequency. Hence, we use this correction method.

The wave equation is typically transferred to the Helmholtz equation which may be solved with a Green's function approach. To yield the electric field, the resulting Green's function G is convoluted with the function f which is essentially the temporal partial derivative of the source current density ($f \propto \mu \partial_t J$):

$$\widehat{E}(\vec{x}, \omega) = \int d\vec{x}' G(\vec{x}, \vec{x}', \omega) f(\vec{x}', \omega). \quad (1)$$

Similar to Bleistein (1986), also other authors, e.g., Miksat et al. (2008), propose Green's functions for a 3D point source and a 3D line source (in x -direction) which corresponds to a 2D point source. These Green's functions may be transferred into each other in the frequency domain using a correction factor $C_\omega(\omega)$ via

$$\widehat{G}^{3D}(\vec{x}, \vec{x}', \omega) = \widehat{G}^{2D}(\vec{x}, \vec{x}', \omega) \cdot C_\omega(\omega). \quad (2)$$

This correction factor is given by $C_\omega(\omega) = \sqrt{\frac{|\omega|}{2\pi\sigma_c}} \exp(-\frac{i\pi}{4} \text{sign}(\omega))$, where σ_c denotes the integral of the velocity with respect to the length s of the ray trajectory $\sigma_c = \int c(s) ds$. Since this correction factor is spatially constant, it may also be used to directly scale the Fourier transform of the electric field:

$$\widehat{E}^{3D} = \int dx dy dz \widehat{G}^{3D} f \quad (3)$$

$$= \int dx dy dz \widehat{G}^{2D} C_\omega(\omega) f \quad (4)$$

$$= C_\omega(\omega) \int dx \int dy dz \widehat{G}^{2D} f \quad (5)$$

$$= C_\omega(\omega) \int dx \widehat{E}^{2D} \quad (6)$$

$$= C_\omega(\omega) C_i \widehat{E}^{2D}. \quad (7)$$

This exploits that (i) the wave propagation is a linear problem in order to separate $C_\omega(\omega)$ and (ii) that the shape of the wave does not change in x -direction due to symmetry. Thus, the integration over the x -direction leads to the constant C_i (m). This the constant is independent of the frequency and hence does not change the electric field in the inverse Fourier transformation. Therefore, it is possible to directly scale the Fourier transform of the electric field with C_ω and to use the normalized amplitude of

the electrical field in the space domain. Thus, the value of the constant C_i is irrelevant. By separating the frequency and amplitude correction in the previous version of the manuscript, we set $\sigma_c = 1$ in the frequency correction and applied the correct value in the amplitude correction. We clarified section 2.1 as well as the normalization in the revised version of the manuscript (P9 L4ff, P9 L15f, P10 L4f, P10 L21f).

The first reflection is not always the one with the highest amplitude (see Figs. 13b and 16b – if the event has the maximal amplitude in both the simulation and the measurement, it has no error as both values are equal to 1, thus you can check that the event with maximal absolute amplitude is not always in the same reflection). The characteristics of the first reflector does change over the course of the experiment, due to the hydraulic dynamics (e.g., see marker (3) at Fig. 9).

A flowchart was added in the revised version of the manuscript (Fig. 3). Besides the 2D to 3D conversion and the event selection, simulated and measured data are treated the same.

2. Neglecting dielectric losses. I'm wondering if at frequencies of about 400 MHz, the impact of free water relaxation can be neglected and whether the imaginary part of permittivity has to be taken into account. When using complex permittivity of water according to Kaatze et al. (1989) and the CRIM formula and a DC conductivity of 0.003 S/m this results in: 3 dB/m (2 dB/m from free water relaxation, 1 dB/m from DC conductivity) for 10vol% water content and 5 dB/m (4 dB/m from free water relaxation and 1 dB/m from DC conductivity) for full saturation (40vol% water content). This means that up to 80% of total loss is caused by polarisation effects of free water. Neglecting these effects results in wrong amplitudes of the simulated data and I'm wondering how they can fit to the field data. At the end of the imbibition experiment (water table at -0.6 m) the amplitudes of the lower reflections (1 m saturated material above, i.e. 2 m two-way travel path) should appear to be approximately 8 dB (2.5 times) higher in the synthetic data than in the field data. I suggest to use the true complex permittivity of water at 400 MHz or, if the FDTD code cannot handle complex property values, an effective HF conductivity including both, DC conduction losses and HF polarisation losses.

Reply:

Using the parameters of Kaatze et. al. (1989) and the measurements of Light et. al. (2005) for the direct current conductivity yields the temperature and frequency dependency of the electrical conductivity of pure water shown in Fig. 1 of this reply. Due to the finite measurement time of the TDR traces, they yield an effective estimate of the electrical conductivity which is larger than the direct current conductivity. Hence, we corrected the notation in the revised version of the manuscript (e.g., P6 L13).

3. GPR forward calculation: Why is a 2D FDTD code used for a horizontally layered model? A 1D reflectivity method as e.g. used by Bradford et al., (2014) or a 1D FDTD code would be much more efficient. The power of FDTD is certainly that it can be used for complicated 2D/3D subsurface models and thus for inverting 2D/3D data with an according hydraulic simulation. However, in the presented study only 1D data are used and no outlook is given how to adopt the strategy to 2D or 3D problems. From this it is

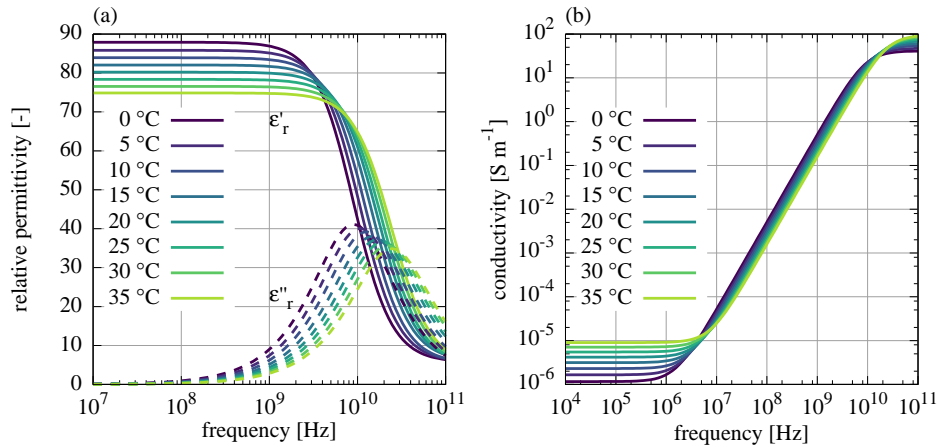


Figure 1: The temperature and frequency dependency of pure water using the parameters of Kaatze et. al. (1989) and the measurements of Light et. al. (2005) for the direct current conductivity.

not clear why the expensive 2D FDTD algorithm is used. The source wavelet of the simulation is different to the wavelet of the experimental data. When dealing with gradient interfaces as the capillary transition zone, the wavelet shape may have a big impact on the maximal amplitude of the reflected signal. Why not using the first reflected signal, which is used for normalisation, as source wavelet in the simulation?

Reply:

In a 1D model, the shape of the wavelet would change, increasing the deviation to the measured 3D antenna signal. Also, using a 1D model would lead to a depth-dependent error in the ray travel path (Fig. 2 of this reply).

We added an outlook on the further application of the proposed algorithm in the revised version of the manuscript (P30 L27ff and P30 L30ff).

Concerning the estimation of the source wavelet, please also note the reply to referee comment 1, point 10.

Inversion. The complex inversion scheme is a nesting of global and gradient methods. It is somewhat nebulous and it's difficult to get an impression of the quality of original data fit. Why do you use different but relatively narrow boundaries (fit ranges) for the inversion parameters of the two layers? By doing this, the inversion result is biased by a-priori information that is usually not known but the actual aim of the investigation. The inversion should work with the same (broader) fit range for both layers. If not, it cannot be adopted to the field. The fit ranges should be used to provide outer boundaries of the deduced material properties in Fig. 9 and Fig. 14. I'm also missing a figure showing experimental GPR data traces and synthetic traces based on the inversion models to prove that the experimental data are well described. This figure should include the resulting synthetic radar traces of the ten best inversion results to get an idea of the

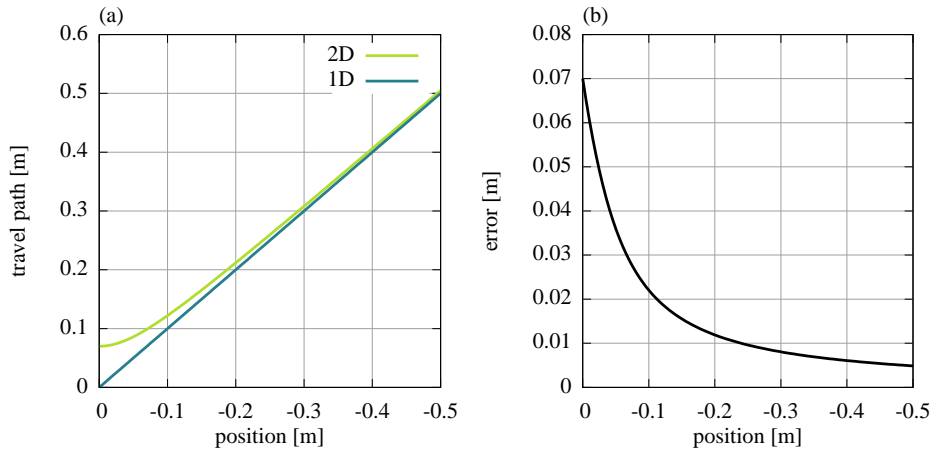


Figure 2: (a) The difference in travel path for 1D and 2D, and (b) the error in travelpath

fluctuations and an idea of the fitting quality.

Reply:

The global-local approach is a common method. It is also typical that larger problems are approached with a preconditioning step.

The deviation in amplitude and travel time as well as the residuals are given in the Figs. 13 and 16.

The fit ranges cover sandy materials. In a field application of the method, the material type of the subsurface can be sampled with a geological drill, e.g., using a "Pürckhauer". The proposed method is intended to be used in combination with published multichannel method Gerhards et. al (2008) and Buchner et. al. (2012) which provide the architecture structure, layer depth, and average water content. These methods have been shown in 2D.

The applied optimization methods use a uniformly distributed prior information. Hence, even if the prior information was included in the cost function, the fit parameter range would not bias the parameter estimation. If the parameter range was too small, the resulting parameters would be close to the boundary. This is not the case in this study. Choosing single traces out of the time-lapse radargram with many traces does not suffice to proof the quality of the fit, because, while the fit might be good for one trace, it could be very bad for other traces. At least in the synthetic study, where there are no additional reflections from the walls and compaction interfaces, the true and the estimated radargrams are very similar. It would be difficult to discern them visually. Thus, we show the evaluated events, their deviations in signal travel time and amplitude as well as the according residuals. This approach allows to pinpoint deviations of the simulation and the measurement very precisely. Hence, showing the 10 best members would require to show 10 plots such as Fig. 13 per study.

5. *In the analysis, the reflection of the compaction layer is excluded. If this interface*

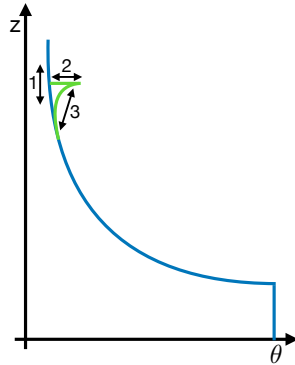


Figure 3: Sketch of the influence of a compaction layer (green) on the water content distribution (blue). Main uncertainties about the shape of the influence are indicated with arrows (1, 2, 3).

causes a GPR reflection, this must be caused by different water contents on both sides and hence, there must be significant differences in the material hydraulic properties (see P24 L25ff). So why should I ignore an interface that is present in the subsurface and reflects changes in hydraulic properties? Please explain.

Reply:

In order to describe the influence of the compaction interface on the water content distribution quantitatively, at least three uncertainties would have to be estimated (Fig. 3 in this reply): The vertical position of the compaction interface (1), the change of the pore-size distribution at the compaction interface (2) as well as the change of the pore-size distribution with increasing distance from the compaction interface (3).

In vertical soil samples taken at ASSESS, e.g., with a Pürckhauer, we could only visually discern the different sands but no compaction interfaces. Since the quantitative influence of the compaction interfaces on the hydraulic dynamics is unknown a priori, we assume homogeneous material properties in this first step, in particular to investigate the necessity for a detailed quantitative analysis of compaction interfaces. Relevance of this representation error is indicated by the structural residuals after the inversion. The results of this study, i.e. the effect on the estimated parameters and the remaining residuals, suggest that the representation of the compaction interfaces in ASSESS is relevant. Hence, we propose that the effect of all relevant representation errors on the estimated properties should be analyzed in a next step, similar as has been done for TDR data by Jaumann and Roth (2017). This is a significant effort well beyond the scope of this paper.

6. The title is misleading, I would suggest to delete "...and subsurface architecture. . ." as this would imply at least a 2D subsurface model. The section headings of 2.2 sound unusual to me. From a geophysical perspective the following headings would give a better description: 2.2.1 Water dynamics, 2.2.2 Hydraulic material characterisation 2.2.3

Time lapse experiment 2.2.4 GPR investigation and electromagnetic material characterisation.

Reply:

We changed the title to "...and layered architecture..." making it more precise. We clarified the introduction of the representation and thus the titles in the revised version of the manuscript (P4 L19ff).

Further comments:

(P2 L27) References are a bit biased by the own workgroup. E.g., when introducing the FDTD method I would expect the basic work of Yee, Taflove. . . and, e.g., the former ETHZ geophysics group or from the gprMax developers.

Reply:

Instead of repeating an extensive list of available literature on the topic, we tried to keep the number of references concise. Hence, we focused on those works that deal with estimation of subsurface properties and that influenced the manuscript. Still, we agree that classical work on methods should be acknowledged and added the references accordingly (P2 L30ff).

(P6 L23ff) The CRIM formula uses the square root of permittivities (see your original reference: Birchak et al., 1974). There is no need to first define a general formulation with an exponent α , which is not the original CRIM formula, and then fix the exponent $\alpha = 0.5$. Keep it simple and use the square root from the beginning.

Reply:

We revised the manuscript accordingly (P7 L3).

Further comments *(P6 L9) You should describe that you use the static permittivity of water (which is acceptable for 400 MHz, at least for the real part of permittivity).*

Reply:

We revised the manuscript accordingly (P6 L16f and P7 L7ff).

(P7 L14) "...removal of the direct and trailing signal". What is the trailing signal? Is this the interference of ground wave, crosstalk, reflection at the ground surface and the antenna metal shielding? In Fig. 3, a part of this trailing signal is remaining, which is confusing. Why not muting this part?

Reply:

We clarified the paragraph accordingly (P7 L21ff).

(P7 L15) ". . . we pick the direct signal and subtract it from the radargram" is confusing. Not the signal is subtracted but the travel time.

Reply:

We revised the manuscript accordingly (P7 L24f).

(P8 L5) "normalized amplitude (original amplitude)". Rephrase, as the amplitude is

either normalized or original.

Reply:

We rephrased the section 2.3.2 accordingly.

(P8 L6) “amplitude is amplified quadratically with travel time” means they are corrected for spherical divergence twice consecutively? Is this just an arbitrary gain function that showed to work well and to correct for spherical and intrinsic attenuation at the specific site? Please explain.

Reply:

This is an arbitrary gain function that showed to work well for the detection of events at lower travel times. This gain function is merely used for the detection, the travel time and amplitude. We clarified the manuscript accordingly (P9 L8ff).

(P11 L3) Eq. 11: I think the expression has to be divided by M to get the classical χ^2 with $\chi^2 = 1$ if the data are described within the error.

Reply:

Since the number of events (M) changes over the course of the optimization, this would lead to a balancing of the number of associated events and the associated residuals. Hence, the association of two events would only be added, if their residual is smaller than the average residual (what is very unlikely). Thus, the optimization algorithm would tend to decrease the number of associated events in order to decrease the cost.

(P11 L4) How is the standard deviation of the normalised travel times and amplitudes calculated, i.e. what are the input data?

Reply:

We added this information to the revised manuscript (P17 L6ff).

(P13 L33) “. . . infinite dipole pointing in x dimension”. This should be y dimension (into the plane of projection). Please provide x,y direction in Fig. 6.

Reply:

We clarified the dimensions by adding them to the labels of Fig. 7.

(P13 L34) a Ricker function is the second derivative of a Gauss-fct, not the first derivative

Reply:

We improved the sentence (P14 L22f).

(P18 L26) What is the meaning of amplitude information of a single channel? You are using a single channel GPR system and only one antenna, so this expression is confusing.

Reply:

We clarified the paragraph (P23 L1ff).

(P24 L30) Couldn't the uncertainty of the groundwater table relative to the ground sur-

face be overcome by simple levelling the ground surface?

Reply:

In principle, this was possible. However, the bottom and the surface ASSESS site is inclined relative to the groundwater level (approx. 0.1 m over the length of the site (Jaumann and Roth, 2017)). Yet, when applying the method in the field, the uncertainty of the position of the groundwater level is also likely to increase with the distance from the well.

(P26 L20ff) is a partial repetition of (P22 L5ff (the lower line 5)).

(P26 L26) “. . . and that (ii) the direct electric conductivity can be assessed with GPR measurements”. I cannot understand the context.

(P27 L13ff) This is again a partial repetition of (P22 L5ff) and (P26 L20ff)

Reply:

We revised the section by deleting the short summary (P27, L27ff).

(P27 L18) Better use “constant offset” (CO) instead of “single-channel” GPR data.

Reply:

In this sentence, we differentiate between single-channel and multi-channel approaches, e.g., used by Buchner et. al. (2012).

(Fig. 3, caption) Are these synthetic or experimental data?

Reply:

These are simulated data. We clarified the caption of Fig. 4 accordingly.

Fig. 6: Which E-field component is shown, what is the x and y direction?

Reply:

The x-component of the E-field is shown. We directions are now given in the labels of Fig. 7.

Fig. 12, bottom: y-axis label: standardized residual: Does 10 mean that the residual is 10 times the STD or should it be 10

Reply:

We clarified the caption of Figs. 13 and 16. It is 10 times the standard deviation, which is for the signal travel time $6 \cdot 10^{-4} \cdot 60 \text{ ns} = 0.36 \text{ ns}$. Hence, 10 times the standard deviation corresponds to 3.6 ns.

Fig. 13: I suggest to split the figure into two individual figures as it might be very confusing to mix the 2D radar section with the time lapse data at one location. The label for the groundwater table reflection is “I” in the upper radar section and “2” in the lower time-lapse data. Actually, it’s very hard to distinguish the label “I” from the label “1” in the upper radar section. Please use the same and distinct labels for the GWT reflection in all figures.

Reply:

Especially for people that are not used to time-lapse radargrams, having a correspond-

ing common offset radargram of the initial state helps to associate the reflections and to understand their temporal evolution.

We clarified the caption of Fig. 14 and increased the size of the markers. Since the groundwater table is fluctuating, Arabic numbers indicate the water induced reflections at different times. Thus, the labels are used consistently in all the figures.

References:

Bleistein, N. (1986). Two-and-one-half dimensional in-plane wave propagation. *Geophysical Prospecting*, 34(5), 686-703.

Buchner, J. S., Wollschläger, U., Roth, K. (2012). Inverting surface GPR data using FDTD simulation and automatic detection of reflections to estimate subsurface water content and geometry. *Geophysics*, 77(4), H45-H55.

Holger Gerhards, Ute Wollschläger, Qihao Yu, Philip Schiwiek, Xicai Pan, and Kurt Roth (2008). "Continuous and simultaneous measurement of reflector depth and average soil-water content with multichannel ground-penetrating radar." *GEOPHYSICS*, 73(4), J15-J23.

Jaumann, S., Roth, K. (2017). Effect of unrepresented model errors on estimated soil hydraulic material properties. *Hydrology and Earth System Sciences*, 21(9), 4301.

Kaatze, U. (1989). Complex permittivity of water as a function of frequency and temperature. *Journal of Chemical and Engineering Data*, 34(4), 371-374.

Light, T. S., Licht, S., Bevilacqua, A. C., Morash, K. R. (2005). The fundamental conductivity and resistivity of water. *Electrochemical and Solid-State Letters*, 8(1), E16-E19.

Miksat, J., Müller, T. M., Wenzel, F. (2008). Simulating three-dimensional seismograms in 2.5-dimensional structures by combining two-dimensional finite difference modelling and ray tracing. *Geophysical Journal International*, 174(1), 309-315.

Yilmaz, O. (1987). Seismic data processing, volume 2 of *Investigations in Geophysics*. Society of Exploration Geophysicists.